International Journal of Engineering & Technology, 7 (4) (2018) 4405-4410

International Journal of Engineering & Technology

Website: www.sciencepubco.com/index.php/IJET
doi: 15840
Research paper

Corrosively of peroxide solutions against conventional and electro less NI-P-CNF/ (tio2-zro2) Nano coatings materials

Manoj Kumar Dhiman [1], Manoj Kumar [1], Munna Ram [1], Sulaxna Sharma [2] *, Awanish Sharma [3]

[1] *Research Scholars Department of Physics, Graphic Era Deemed to be University, Dehradun, UK, India*
[2] *Department of AS&H, THDC, IHET, Tehri, UK, India*
[3] *Department of Physics Graphic Era Deemed to be University, Dehradun, UK, India*
**Corresponding author E-mail: awanish@geu.ac.in*

Abstract

In the present experimental effort, an electroless Ni-P-CNF and the Ni-P-TiO2-ZrO2 nano-composite coatings have been deposited on basic mild steel (grade AISI1400) substrate. For EL Ni-P-CNF coating an amount (5 gpl) of activated CNF nano-particles and for Ni-P-TiO2-ZrO2 a mixture of equal amount (2.5 gpl each) of TiO2/ZrO2 nano-particles were incorporated into an acidic electroless Ni-P bath as a second phase material and were reduced by a reducing agent named sodium hypophosphite. After electroless coating, as-prepared Ni-P-CNF and Ni-P-TiO2-ZrO2 EL depositions were heated at 400 □C in Ar environment for one hour duration and were analysed for surface morphology and elemental composition by FESEM and EDAX methods. A compact, homogeneous and consistent allocation of CNF nano-particles and uniform allocation of TiO2+ZrO2 nano-particles into EL Ni-P matrixes is observed respectively, through results analyses of FESEM and EDAX methods. The long term immersion weight loss corrosion test results in alkaline peroxide solutions anticipated that electroless nano-composite coatings demonstrate better corrosion resistance as against to MS, SS316L conventional steels and analogous to duplex stainless steel 2205. Further, the enhanced peroxide and chloride containing solutions are more corrosive than less peroxide and without chloride solutions.

Keywords: *Electro Less; Coatings; Steels; FESEM-EDAX; Peroxide; E-PH; Corrosion; Etc.*

1. Introduction

The chemical and petrochemical, textiles, polymers as well as the paper industry all are beguiling on non-chlorine chemicals such as oxygen, ozone, hydrogen peroxide and peracids to attempt the reducing toxic wastes. A numerous investigations correlated to corrosive effects owing to peroxide solutions in paper industry being a most versatile industry (pH 2.3-14, temperature 50-900 ^{0}C and chloride up to 2000 ppm) is studied. The one study [1] in paper industry found corrosive consequences of peroxide into chlorine dioxide bleaching solution on 316L stainless steel. The other study in related industry [2] recommended 300 series of stainless steels for dealing peroxide solutions. In yet another studies [3], [4] whilst studying corrosion of titanium (Ti) metals into peroxide solution established that ($MgSO_4$) magnesium sulphate was not a proficient inhibitor. In the other studies [5-7], consequences of chelants on the corrosivity of peroxide solutions are discussed in detail and these studies points out substitution of reactor materials to high-performance SS 904L or duplex SS2205 in tested solutions. Further, increase demand of product (paper) in quantity and quality wise will employ newer chemicals and environments in concerned segments. Consequently, performance of machinery materials will be affected, which in numerous cases will result to exacerbate circumstances. Therefore to avoid such aggravate situations, corrosion investigations on conventional and novel materials/coatings of composition have turn out to be essential in order to envisage metallurgy of equipments into altered circumstances of bleaching stages in paper industry. In recent times, electroless (EL) coatings/composite coatings have put on extensive popularity in petrochemicals, automobiles, space, nuclear, marine, textile and paper industry owing to its capability to produce hard, wear and friction resistant, antibacterial and corrosion resistant surfaces [8,9]. The EL composite coatings can be principally categorized into two clusters: (i) coatings incorporating soft particles (PTFE, MoS_2, HBN and graphite) to improve corrosion resistance, reduced friction coefficient and to endow with better lubricity and (ii) coatings holding stiff particles (Al_2O_3, WC, Si_3N_4, SiC, TiO_2, ZrO_2, CeO_2, CNT, CNF as well as diamond) for receiving higher hardness, wear, friction and corrosion resistance [10]. Among above particles, carbon nano fibers (CNFs) have a unique combination of properties, such as extremely high specific strength, stiffness, good heat, corrosion, wear resistance, light-weight, and good thermal and electrical conductivities on the other hand TiO_2 and ZrO_2 nano particles have mostly all above properties except high temperature corrosion and wear resistance and antibacterial activity.

The above all properties enable CNF, TiO_2 and ZrO_2 nano particles to be widely used in paper, chemical, aircraft, automobile, nuclear and electronics industries. Therefore, Ni-P-CNF and Ni-P-TiO_2-ZrO_2 new nano-composite coatings have been prepared by EL method and efforts are made to perform a long term corrosion test and to check suitability of mild steel, stainless steels (austenitic and duplex grade) and above new EL coated nano-composite materials in bleach plant peroxide solutions. The (E-pH) potential –Pourbaix diagram is also constructed for H_2O_2-H_2O system with a view to help in understanding the corrosion protection/ reactions taking place in the present solution compositions and concentrations.

2. Experimental details

2.1. Materials selection and preparation

The test materials for corrosion investigation were selected on the basis of their current use and their possible uses in future bleach plants of paper industry. Accordingly, mild steel (MS, AISI 1400), austenitic stainless steel (SS316L), duplex stainless steel (SS2205) and EL coated Ni-P-CNF; Ni-P-TiO_2-ZrO_2 nano-composite materials were opted for the long term weight loss corrosion test. The dimensions of flat coupons for long term weight loss corrosion test are selected as 20 mm × 20 mm × 4 mm. The composition of the stainless steels for flat coupons is shown in Table 1. For substrate sample preparation, shaping, parting, milling and surface grinding course of action are adopted [11]. After above processes, substrate surface is mechanically cleaned by distilled water and a pickling action is lay down with dilute (50 %) HCl for diminutive time to get rid of any surface rust pursue by rinsed with distilled water and methanol cleaning [11]. The glowing polished, cleaned sample was then immersed in 1% aqueous solution of $SnCl_2$ (2-3 drops of 1M HCl was added to dissolve $SnCl_2$) for 40 seconds to activate the substrate face. The substrate sample was subsequently washed by resources of distilled water and air dried. Soon after the substrate sample is vertical active by dipping it into a mild hot palladium chloride solution (55°C, $PdCl_2$) for a very short duration followed by washing with distilled water and air dry. Now the well activated substrate sample is dipped into EL bath solution retain at 80 to 85 °C and Ni-P-CNF, Ni-P-TiO_2-ZrO_2 nano-composite coatings are deposited in two hours. The composition, concentration and operating parameters for EL Ni-P-CNF, Ni-P-TiO_2-ZrO_2 nano-composite coatings are conferred in Table 2.
Coating thickness is calculated by way of following formula-

Coating thickness (µm) = W x 10^4 D x A

Here 'W' put down for weight increase (g), 'D' is density of deposits (7.75 g/cm^3) and 'A' is surface area of deposition (cm^2). The plating speed (µm/h) was measured as thickness of deposition set down per unit time of deposition [12]. For the present work, coating thickness is established in variation of 20 to 47 µm. When coating is over, coated coupons are washed by distilled water and dried in air. To make out the conclusion of heating on corrosion resistance of EL nano-composite coatings, coated coupons are annealed in furnace for 1 hour period at temperature 400 °C in Argon (Ar) atmosphere. Consequent to annealing, coated coupons are cooled to room temperature and are used for different tests.

Table 1: Composition of Test Material for Weight Loss Corrosion Test

Plate Samples										
Alloys	C	Cr	Ni	Mo	P	Cu	Mn	S	Si	N
MS	0.18	-	-	-	-	-	1.66	-	0.04	-
SS316L	0.019	17.43	11.26	2.03	0.027	0.40	1.11	0.002	0.50	0.048
SS2205	0.022	22.13	5.55	3.16	0.02	0.21	1.47	0.001	0.35	0.188

Table 2: Electro Less Bath Components and Their Function

S. No.	Salt/Compound chemical formula	Quantity in gram (g) for 100 ml	Function of chemicals
1	Nickel Sulphate ($NiSO_4$)	3.52 g	Source of Ni^{2+} ions
2	Trisodium Citrate	4.8 g	Complexing agent, prevent uncontrolled release of Ni^{2+} ions
3	Sodium Acetate	2.2 g each	Work as basic buffer in the presence of ammonia, to maintain the pH
4	Sod. Hydroxide/ Acetic acid10% Solution	Added drop wise	Maintain pH of the solution ~5.5
5	Sodium Hypophosphite	2.1 g	Reducing agent, provide electrons to the Ni^{2+} ions which on accepting electrons get reduced to Ni^0 and deposited on the catalytic surface
6	Sodium Dodecyl Sulphate	0.01g	increase the wettability and surface charge
7	Lead Acetate	0.1mg	Stabilizer
8	Synthesized ZrO_2	0.25g	Work as reinforcement into the matrix
9	Synthesized TiO_2	0.25g	Work as reinforcement into the matrix
10	Synthesized CNF	0.5g	Work as reinforcement into the matrix
10	Bath Operating Conditions	-	pH 5.5; Temperature 85-90 °C; constant rousing is required
11	Annealing Hotness	Up to 400 ^{0}C	Understand the consequence of heat conduct on corrosion resistance

2.2. Solutions for corrosion tests

All well prepared flat samples are exposed into (H_2O_2) peroxide media having alkaline pH (= 9.5) with subjective Cl^- and peroxide concentration. Intended for making peroxide solutions, 50% H_2O_2 Analar grade chemical is considered. The peroxide solution was uniformly mixed into distill water in requisite quantity so as to contain 250 ppm H_2O_2 in addition to 500 ppm H_2O_2 as well as their pH was accustomed to 9.5 employing 10% NaOH solution. The NaCl was poured into solutions for having most wanted level of Cl^- ion amount. Further composition of test solutions was analyzed for H_2O_2, Cl^- as well as pH employing respectively customary method [12] and pH meter. Below Table 3 illustrates chemical composition of peroxide test solutions.

Table 3: Chemical Composition of Peroxide Test Solutions for Weight Loss Corrosion Test (Ph = 9.5)

Chemicals	Solution 1	Solution 2	Solution 3	Solution 4
Peroxide (ppm)	250	250	500	500
Chloride (ppm)	0	400	0	400

2.3. Corrosion test

The long term weight loss immersion corrosion experiment is carried out for corrosion rate assessment, where well cleaned weigh up test specimens were exposed for six months time at room temperature (27 to 38 ^{0}C). Each one coupon was fitted by serrated washers for commencing crevice corrosion and is immersed into test solutions as mentioned in Table 3. During the immersion test, H_2O_2, Cl^- and pH of solutions were examined and keep up one time in a week. Throughout the test phase, quantity of H_2O_2 decreased (5% to 12%), Cl^- decreased (1.1% to 4.3%) and pH decreased (2.5 to 4 %) of individual initial mark values. After six month exposure, corroded specimens were cleaned mechanically pursued by dealing with cold solution of concentrated HCl with 20 g/L $SbCl_3$ and 50 g/L $SnCl_2$ [13]. Corroded specimens were then weighed for estimating weight loss so as to establish corrosion rate by means of subsequent formula:

Corrosion Rate (mpy) = 3.45 x 10^6 × W D T A

Where 'mpy' is mils per year, 'W' is weight loss in grams, 'D' is density of metal in gm/cm^3, 'T' is exposure time in hours and 'A' is area in cm^2.The corroded along with cleaned specimens were examined underneath optical metallurgical microscope (Riechert Jung, USA make) for evaluating pitting and crevice corrosion attack by measuring utmost depth of attack upon open surface along with under serrated washer area of coupon respectively.

2.4. Analysis of coatings

The microstructure and constituent composition of as-plated in addition to heat treated specimens were intended by the help of FESEM and EDAX techniques. Their X-ray diffraction (XRD) study was carried out by source of Cu K_α X- rays for identifying phases present. The sufficient grain dimensions of the deposit were calculated by using Scherer equation ($t = 0.9\lambda / B\cos\theta_B$) where parameter λ is Cu K_α wavelength (λ=1.54 Å), B is broadening of full width at half maximum furthermore θ_B is the Bragg's angle by intense Ni (111) peak (after removal of instrumental broadening cause) [14-19].

3. Results and discussion

3.1. Characterization of coatings

The FESEM and EDAX micrographs of the representative coated samples are shown in (Fig. 1a, 1b, 2a and 2b). FESEM of as-plated EL Ni-P-CNF EL nano-composite coated coupon have compact, amorphous and uniform structure with fiber diameter of roughly 15 to 90 nm range. When the EL nano-composite coated coupons are heated at 400 ^{0}C for one hour under Argon atmosphere, the globules of nickel and phosphorus with well dispersed CNF nano-particles turn out to be more close packed, fiber diameter increases which condensed porosity of coatings (Fig. 1a). The small quantity of surfactant (Sodium dodacyl Sulphate i.e., SDS) and activation of CNF nano-particles into Ni-P electroless bath is thought to be the main reason for homogenous allocation of CNF nano-particles on to base surface.

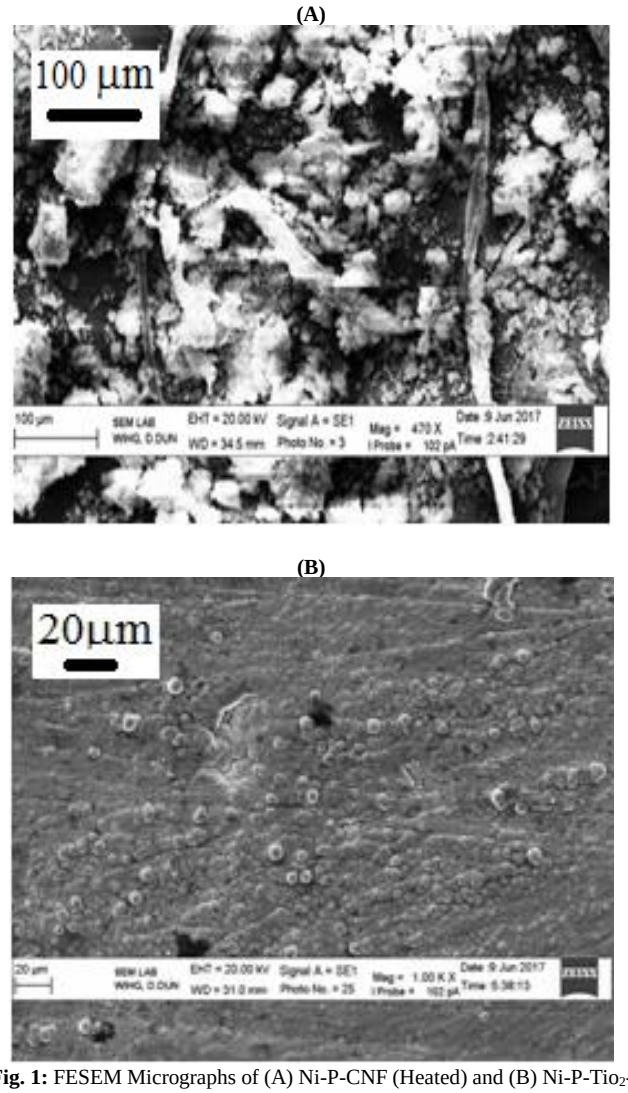

Fig. 1: FESEM Micrographs of (A) Ni-P-CNF (Heated) and (B) Ni-P-Tio$_2$-Zro$_2$ (Heated) Nano-Composite Coatings.

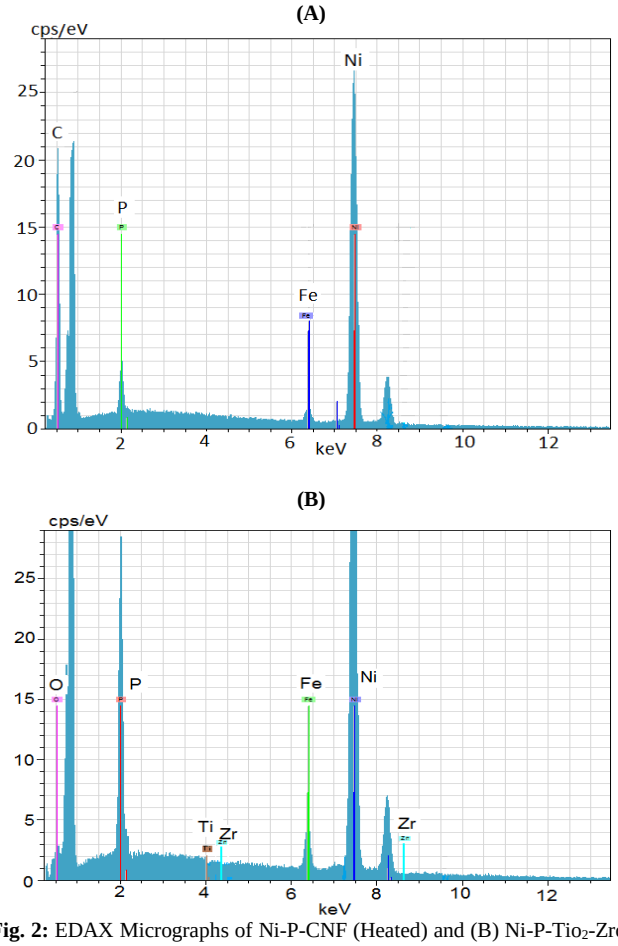

Fig. 2: EDAX Micrographs of Ni-P-CNF (Heated) and (B) Ni-P-Tio$_2$-Zro$_2$ (Heated) Nano-Composite Coatings.

The developed EL Ni-P-CNF nano-composite coating were examined under as-plated and heat treated conditions by EDAX analysis (Table 4; Fig. 2a). It is also noticeable from the EDAX analysis that quantity of coating element Ni, P and C decreases on heating while that of Fe increases. This result can be possible because of dispersion of coating element towards interface of plating plus substrate surface and may cause increased corrosion in heat treated case [18,19] .The XRD patterns (Fig. 3) of Ni-P-CNF (As-plated) EL nano-composite coatings reveals that coating is amorphous in character as broad and small peak is available at the diffraction angles (2θ) 24.9^0 and other wide peak is available at the diffraction angles (2θ) 44.2^0 (JCPDS card no. 75-1621for C and JCPDS 75-2078; CNF). The single broad peak is a proposition of Ni-P alloy. The FESEM/EDAX micrographs of Ni-P-CNF (As-plated) coupons authenticate the presence of CNF nano-particles into Ni-P matrix. Although, the diffraction peak corresponding to CNF nano-particle is very small in XRD pattern, it can be because of low quantity and high distribution of CNF nano particles into EL Ni-P matrix. The XRD pattern of heated (400°C) Ni-P-CNF coating demonstrates the transformation of amorphous phase into typical crystalline phase. The flap peak of CNF appears at approximately 25.3^0 which are coidentical with the graphite. Apart from this a peak of Ni_3P phase is also observed for the coating. Peaks of Ni are observed at diffraction angles of 52.6^0 and 76.5^0 (JCPDS 01 to 1260; FCC Ni) and for Fe as a substrate at 36.3^0 and 65.1^0 (JCPDS 13-0534; Fe).The uppermost peak of Ni_3P is observed at diffraction angle of 44.2^0 (JCPDS 34 to 0501; BCC Ni_3P). The evidence identical to (111), (200) plus (220) planes, FCC phase of Ni can be experienced. On heat treatment the grains get roughen which assist in growing hardness plus wear resistance of depositions [17-20. The low quantity plus high dispersion of CNF nano-particles into EL Ni-P medium is responsible for small peaks as well as Ni-P peaks are not shifted. The breadth of main peak of Ni (111) point out grain proportions are in range of 6 to 15 nm [16–24].

Table 4: EDAX Analysis of Ni-P-CNF/ Ni-P-Tio_2-Zro_2 Nano-Composite Coatings

Element	Weight %			
	Ni-P-CNF As-Plated	Ni-P-CNF Heat-treated	Ni-P-TiO_2-ZrO_2 As-Plated	Ni-P-TiO_2-ZrO_2 Heat-treated
Ni K	85.61	84.32	81.45	79.65
P K	10.74	10.38	11.49	10.19
Ti K	-	-	0.56	0.41
Zr K	-	-	0.46	0.32
O K	-	-	3.21	3.14
Fe K	2.03	3.71	2.42	4.76
C K	1.62	1.59	0.13	0.12
Total %	100	100	100	100

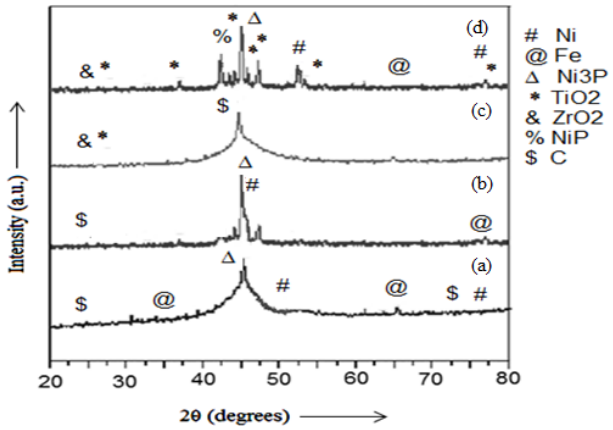

Fig. 3: XRD Patern of (A) Ni-P-CNF (As Plated) (B) Ni-P-CNF (Heated) (C) Ni-P-Tio_2-Zro_2 (As Plated) And (D) Ni-P-Tio_2-Zro_2 (Heated) Nano-Composite Coatings.

The results from XRD, FESEM-EDAX study on Ni-P-TiO_2-ZrO_2 as-plated and Ni-P-TiO_2-ZrO_2 400^0C coated surface are shown in (Figs. 1b, 2b, 3c and 3d) suggests that, inclusion of TiO_2 and ZrO_2 nano-particles into EL Ni-P matrix results in change in coated surface and with roughly uniform distribution of TiO_2 and ZrO_2 nano-particles over the coated surface with measurable density. The consistent distribution of TiO_2 and ZrO_2 nano-particles on surface may be due to presence of very low quantity of surfactant (SDS) in the acidic Ni-P EL coating unit. For heat treated coupon at 400^0C for 1h, the gobbets of nickel as well as phosphorus through deep-rooted TiO_2 along with ZrO_2 nano-particles turn out to be more packed in, which reduced porosity of the nano-coatings and this result is also in accordance [10, 21-25]. This may get better corrosion resistance of EL nano-composite coatings.

In EDAX spectra of Ni-P-TiO_2-ZrO_2 EL nano-composite coatings besides Ni and P peaks, the very weak peaks of zirconium and titania are also observed. Though the peaks are very weak but suggest the co-deposition of zirconium plus titania nano- element into EL Ni-P medium. In Ni-P-TiO_2-ZrO_2 as-plated deposition, the phosphorus (P) amount, to some extent is elevated than Ni-P-TiO_2-ZrO_2 heat treated. The higher P content can prevent the nucleation of Ni (f.c.c.) phase which outcomes as amorphous configuration with higher fineness and density of surface structure than Ni-P-TiO_2-ZrO_2 heat treated. It is marked from the EDAX analysis that the amount of Ni, O, zirconia and titania particles also decreases in case of Ni-P-TiO_2-ZrO_2 heated coating in contrast to Ni-P-TiO_2-ZrO_2 as-plated coating. The EDAX examination reveals that considerable quantity of iron is headed for dispersal depositions into edges of depositions and substrate. This may fallout in an augmented corrosion [10], [13], [21-30]. However, in Ni-P-TiO_2-ZrO_2 as-plated EL nano-composite coatings a smaller amount of iron put forward less diffusion of plating which may support in prevention of corrosion.

The XRD plots of EL Ni-P-TiO_2-ZrO_2 nano-composite coatings are shown in Fig. 3 as-plated and heat treated at 400 °C. These Figs. divulge that phase of as-plated coupon is roughly more amorphous than crystalline and a solitary extensive peak is existing at diffraction angle of 44.2^0 (Ni) plus other very low peaks are available at angle of 28.1^0 (JCPDS00-024 to 1164, 01 to 078-0047; ZrO_2) [26-30] and 28.4^0 (JCPDS 01-074-0508 to 01-071-1166; TiO_2). It can be because of co-deposition of TiO_2 and ZrO_2 nano-particles with high distribution and in very less amount into the EL Ni-P matrix. Secondly for heat treated coupon (400 °C) more nebulous nature of coatings gets transformed into semi-crystalline (more crystalline less amorphous) nature with crest on different diffraction angles.

The topmost peak of Ni_3P with TiO_2 is experienced for diffraction angle 44.2^0. The Ni-P peaks are experienced at 42.1^0, 44.76^0 plus 45.14^0. The TiO_2 peaks are experienced at 35.2^0, 53.46^0, 57.7^0 and 77.28^0 diffraction angles. The Ni diffraction peaks at 52.11^0, 76.5^0 and Fe diffraction peaks are experienced as a substrate at 64.5^0. Interestingly ZrO_2 peaks are not observed in case of heat treated case this can be because of very low amounts of ZrO_2 nano-particles into matrix of EL Ni-P. It is also thought that dispersion distributed ZrO_2 nano-particles have good resistance to high temperatures, which can control the oxidation of the composite coatings and put off the growth of crystal grains and re-crystallization. Thus degree of crystallization and oxidation of EL Ni-P-TiO_2-ZrO_2 heat treated coating was decreased.

The reflections corresponding to (111), (200) and (220) planes, the fcc phase of Ni is able to be pragmatic. The Ni_3P (bcc) alloy phase is accountable in favor of strengthen in hardness and wear confrontation of coatings [10-17], [20-24]. The grains dimension of depositions is roughly within the range among 3.27 nm to 13.46 nm. In XRD spectra of Ni-P-TiO_2-ZrO_2 as-plated and heat treated depositions, the Ni-P peak does not carry out any major shift because of incorporation of nano-particles in little concentration as compared with basic EL Ni-P depositions. Hence consequences attained here are into good accordance through the outcome reported by [21-26] and breadth of foremost crest of Ni (111) point out grain proportions of coatings are in range among 3.2-16.9 nm for as-coated and heat treated samples. Observations [7-12], [15-25] also confirm it.

3.2. Corrosion investigations

It is worth mentioning to recognize different chemical reactions which are accountable for corrosion of materials into peroxide solutions. Further it is also necessary to have information about chemicals varieties exist into peroxide solutions. For this reason an E-pH (Pourbaix) diagram was build for H_2O_2-H_2O system by using different equations as given in reference [30], which is very similar to the diagram as reported in [31]. For obtaining these equations, quantity of H_2O_2 was taken as 250 ppm as well as 500 ppm, similar as into test solutions. The following equilibrium (Eqn. (i)) suggest the closeness of lines 4 and (4) in the E-pH (Fig.4) diagram

$$H2O2 \leftrightarrow O2 + 2\ H+ + 2\ e- \quad (i)$$

Here from above reaction it is concluded that O_2 is reducing to H_2O_2 and H_2O_2 oxidizing to O_2. Further a peroxide solution at the pH 9.5 (test solution pH) value will have H_2O_2 and O_2 as main chemicals. These chemical species will also be liable for subsequent reduction reactions (Eqn. (ii and iii)) e.g.

$$H_2O_2 + 2\ H^+ + 2\ e^- \rightarrow 2\ H_2O \quad (ii)$$

$$O_2 + 4H^+ + 4\ e^- \rightarrow 2\ H_2O \quad (iii)$$

Owing to elevated potential of H_2O_2 reduction reaction, the H_2O_2 will take over in controlling corrosion of steels into peroxides. These consequences will further enhance the pH of the solution. The raise into pH was also experienced whilst monitoring weight loss corrosion test.

Corrosion rates of steels into different peroxide solutions are specified into Table 5. One scrutinizes peroxide solution devoid of Cl^- to be least corrosive furthermore those with Cl^- are more corrosive. Moreover, amplified H_2O_2 amount illustrates elevated corrosion rates upon individual materials. Accordingly raise in H_2O_2 and Cl^-

amount into solutions formulate peroxides with extra corrosivity. The Table 5 illustrates degree of pitting as well as crevice corrosion attack on various coupons into test solutions. According to this table, every two kind of localized attack are originated while the solutions left with elevated H_2O_2 and Cl^- amount. Therefore, peroxide solution with no chloride and 250 ppm peroxide is least corrosive while that with 400 ppm chloride and 500 ppm peroxide shows highest degree of corrosivity and localized corrosion attack. It is found that as H_2O_2 and Cl^- amount enhanced the increased corrosivity of solutions may be assigned to H_2O_2/ H_2O reaction (Eqn. (iv)). The Nernst equation is specified as

$$EH2O2 = 1.776 - 0.059\ pH + 0.0295 \log [H2O2] \quad (IV)$$

Increase in concentration of H_2O_2 will shift E_{H2O2} to upper values by this means escalating OCP as well as corrosion rate of the metal. While enhanced corrosion owing to larger level of Cl^- could be ascribed to reduce passivation range of stainless steels, which in twirl will augment corrosion rate. Therefore corrosivity of peroxides is expected to boost by means of augmented peroxide plus chloride levels which may be an outcome in case of filtrate recycling.

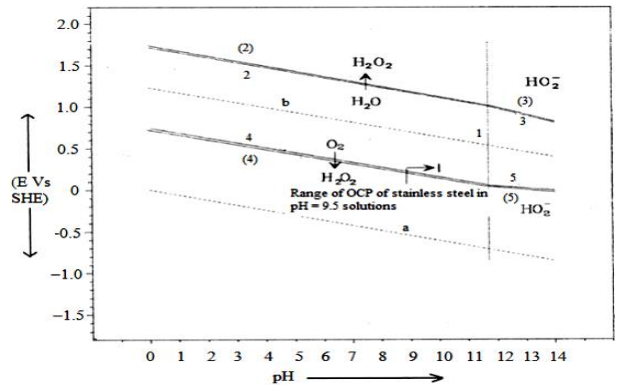

Fig. 4: E-Ph Diagram for H_2O_2/H_2O System at Room Temperature.

Table 5: Corrosion Rate (MPY*) of Test Coupons in Peroxide Solutions (PH = 9.5)

Alloys	Parameters	Solution 1	Solution 2	Solution 3	Solution 4
MS	Corrosion rate (*mpy)	5.89	6.43	6.51	6.87
	Pitting attack(µm)	#NMA	10	#NMA	13
	Crevice attack(µm)	20	22	25	27
SS 316L	Corrosion rate (mpy)	0.22	0.21	0.31	0.28
	Pitting attack(µm)	23	25	28	31
	Crevice attack(µm)	23	30	24	33
Ni-P-CNF (As-plated)	Corrosion rate (mpy)	0.27	0.30	0.33	0.40
	Pitting attack(µm)	20	25	23	30
	Crevice attack(µm)	20	24	23	32
Ni-P-CNF (Heated)	Corrosion rate (mpy)	0.29	0.26	0.42	0.49
	Pitting attack(µm)	24	27	28	33
	Crevice attack(µm)	21	24	21	30
SS2205	Corrosion rate (mpy)	0.001	0.002	0.01	0.10
	Pitting attack(µm)	$NVA	10	10	13
	Crevice attack(µm)	$NVA	$NVA	$NVA	10
Ni-P- TiO_2-ZrO_2 (As-plated)	Corrosion rate (mpy)	0.24	0.27	0.31	0.35
	Pitting attack(µm)	20	23	21	38
	Crevice attack(µm)	18	20	20	29
Ni-P- TiO_2-ZrO_2 (Heated)	Corrosion rate (mpy)	0.26	0.23	0.37	0.42
	Pitting attack(µm)	21	25	28	32
	Crevice attack(µm)	21	22	24	29

* MPY – mils per year, $NVA –No visible attack, #NMA- No measurable attack.

According to Table 5, corrosion rates (in mpy) are experienced to differ as per subsequent mode: MS > Ni-P-CNF (Heated) > Ni-P-CNF (As-plated) > Ni-P-TiO_2-ZrO_2 (Heated) > Ni-P-TiO_2-ZrO_2 (As-plated) > SS316L > SS2205

Some representative images of samples after weight loss test are shown in Fig. 5 (a-c). In bulk of cases, duplex SS 2205 demonstrate superior performance. The inclination is as per chemical composition of test materials. From the Table 5, MS is experiencing merely uniform and crevice corrosion whilst very less pitting is experienced in other two solutions. A motivating observation is that Ni-P-TiO_2-ZrO_2 coatings show slight better than SS316L and Ni-P-CNF coating in terms of pitting and crevice corrosion attack. The other notable observation is that Ni-P-CNF (As-plated) is set up to act upon slight enhanced than SS 316L and Ni-P-CNF (Heated) in terms of pitting and crevice corrosion attack. Localized corrosion attack on duplex SS2205 is experienced the smallest amount (Table 5). Thus by and large, different materials on the basis of weight loss test, may well be graded in stipulations of their resistance next to uniform as well as localized corrosion in the comportment: SS2205 > Ni-P-TiO_2-ZrO_2 (As-plated)> Ni-P-TiO_2-ZrO_2 (Heated) > Ni-P-CNF (As-plated) > SS316L ~ Ni-P-CNF (Heated) > MS.

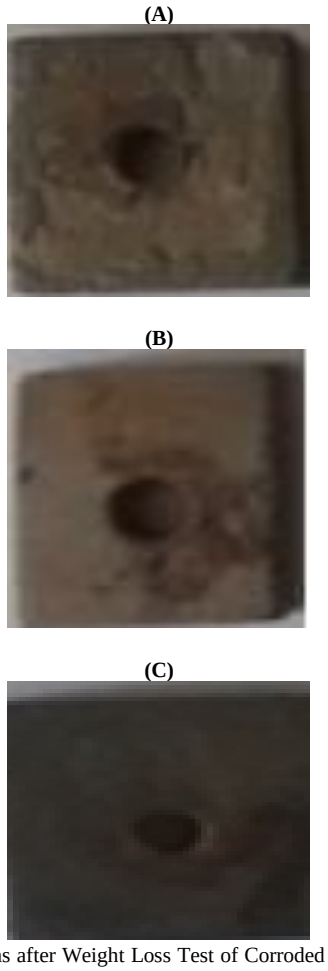

Fig. 5: Photographs after Weight Loss Test of Corroded Coupons (A) MS Coupon (B) Ni-P-Tio_2-Zro_2 (As Plated) and (C) Ni-P-CNF (Heated).

4. Conclusions

The appearance of Ni-P-CNF coatings is blackish type while that of Ni-P-TiO_2-ZrO_2 coatings is greyish white type. The XRD/SEM examinations illustrate that EL Ni-P-TiO_2-ZrO_2(As-plated), Ni-P-CNF (As-plated) depositions have amorphous nature; while EL Ni-P-TiO_2-ZrO_2 (Heated) Ni-P-CNF (Heated) materials demonstrate decline in amorphous nature and enrichment in crystallization nature. These transformations propose to elevate hardness plus wear resistance in coated heated coupons. The heated Ni-P-TiO_2-ZrO_2, Ni-P-CNF EL depositions depict less corrosion resistance in compare to as-plated coupons; even though it is far improved than MS and SS316L coupons. Consequently heated depositions can be recommended for application in cases where obligation is for enhanced triobological qualities along with not so corrosive environment. The Ni-P-TiO_2-ZrO_2 coatings reveal slight better corrosion resistance than Ni-P-CNF EL depositions. Among all materials, a comparison of overall material performance against corrosion attack still indicates the best material to be SS2205. The electrochemical study of these coatings will reveal a better picture. The better cost/strength ratio of SS2205 creates it more apposite for managing peroxide media with/without Cl^- amount than other tested coupons.

References

[1] D. C. Bennett, Cracking of continuous digester-review of history, Corrosion, 40(1983) 1-4. https://doi.org/10.5006/1.3579290.

[2] R. Bloom, L. E. Weeks, C. W. Rayleigh, *Corrosion* Comparisons between zirconium and titanium, Corrosion, 16 (1960) 164.

[3] O. A. Hyökyvirta, Experimental determination of the Critical hydrogen peroxide ion concentration for titanium alloys in alkaline hydrogen peroxide solution, Corrosion Science and Technology, 48 (1997) 376-387, 1997.

[4] W. E. Wyllie, B. E. Brown, D. J. Duquette, Mechanism of action of Simons' stain, Tappi journal, 78 (1995) 151.

[5] A. Garner, Avesta Stainless Steels for Chemical Pulp Bleach Plants, Information 9063:2, 14 (2002) [3].

[6] A. Delblanc, L. Lundberg, Experience of Stainless Steels in Pulp and Paper Mills Part-1, Paper Asia Journal, 19 (2003) 21-24.

[7] Rohtash, A. K. Singh, R. Singh, Corrosion Study of Stainless Steels in Peracetic Acid Bleach Media with and without Chloride and Chelant, International Journal of Research and Innovations in Science and Technology, 1 (2014)1-10.

[8] R. Kumar, S. Sharma, A. Sharma, Corrosion study of Electroless Ni-P-Al_2O_3-ZrO_2 Nanocomosite coatings in paper mill digester, Indian Journal of Science and Technology, 9 (2016) 1-8. https://doi.org/10.17485/ijst/2016/v9i44/98981.

[9] R. C. Agarwala, V. Agarwala, R. Sharma, Electroless Ni-P Based Nanocoating Technology—A Review, Synthesis and Reactivity in Inorganic, Metal-Organic, and Nano-Metal Chemistry, 36 (2006) 493-515. https://doi.org/10.1080/15533170600596030.

[10] S.B. Sharma, Synthesis and triobological characterization of Ni-P based electroless composite coatings, Ph.D. Thesis, IIT Roorkee, 2002.

[11] ASTM G1-10, "Preparing, cleaning and evaluating corrosion test specimens" 03(1991) 02.

[12] A. I. Vogel, Quantitative Inorganic Analysis, London, Longman, Green & Co., Ed. 1964, pp. 296.

[13] A. Sharma, A.K. Singh, Electroless Ni-P and Ni-P-Al_2O_3 Nanocomposite Coatings and Their Corrosion and Wear Resistance, Journal Material Engineering and Performance, 22 (2013) 176-183. https://doi.org/10.1007/s11665-012-0224-1.

[14] G. Singh, Corrosion Investigation on Materials in Bleach Media of Paper Industry, Ph.D. Thesis IIT-Roorkee, 2003.

[15] A. Sharma, Corrosion Investigations in Pulping and Bleaching media, PhD. Thesis, Indian Institute of Technology Roorkee, 2006.

[16] S.B. Sharma, R.C. Agarwala, V. Agarwala, Development of electroless composite coatings by using in-situ co-precipitation followed by co-deposition process", Metallurgical and Materials Transactions, 36B (2005) 23-31. https://doi.org/10.1007/s11663-005-0002-7.

[17] P. Gillespie, Electroless Nickel Coatings: Case study, Surface Engineering casebook, edited by J.S. Burnell-Gray and P.K. Datta, Woodhead Publishing limited, 1996, 49-72.

[18] L.M. Ang, T.S.A. Hor, G.Q. Xu, C. Tung, S. Zhao, J.L.S. Wang, Electroless Plating of Metals onto Carbon Nanotubes Activated by a Single-Step Activation Method, Chemical Materials, 11 (1999) 2115-2118. https://doi.org/10.1021/cm990078i.

[19] Z. Yang, H. Xu, Y.L. Shi, M.K. Li, Y. Huang, H.L. Li, The fabrication and corrosion behavior of electroless Ni–P-carbon nanotube composite coatings, Material Research Bulletin, 40 (2005) 1001-1009. https://doi.org/10.1016/j.materresbull.2005.02.015.

[20] J. Novakovic, P. Vassiliou, Kl. Samara, Th. Argyropoulos , Electroless NiP–TiO_2 composite coatings: Their production and properties, Surface Coating Technology, 201 (2006) 895-901. https://doi.org/10.1016/j.surfcoat.2006.01.005.

[21] A. Zielinska, A. Stankiewicz, I. Szczygiel, Electroless deposition of Ni-P-nano-ZrO_2 composite coatings in the presence of various types of surfactants, Journal of Colloid and Interface Science, 377 (2012) 362–367. https://doi.org/10.1016/j.jcis.2012.03.049.

[22] M. A. Kumar, R.C. Agarwala, V. Agarwala, Synthesis and characterization of electroless Ni–P coated graphite particles, Bulletin Material Science, 31 (2008) 819–824. https://doi.org/10.1007/s12034-008-0130-1.

[23] S. Rossi, F. Chinni, Corrosion Protection Properties of Electroless Ni/PTFE/ Phosphate/MoS_2 and Bronze/PTFE Coatings Applied to Improve the Wear Resistance of Carbon Steel, Surface Coating Technology, 173 (2003) 235-242. https://doi.org/10.1016/S0257-8972(03)00662-5.

[24] J.N. Balaraju, T.S.N. Sankara Narayanan, S.K. Seshadri, Structure and phase transformation behaviour of electroless Ni–P composite coatings, Materials Research Bulletin, 41 (2006) 847–860. https://doi.org/10.1016/j.materresbull.2005.09.024.

[25] F. Lin, J.C. Lian, K.Y. Li, The effect of electroless nickel film on the tribological characteristics of alumina coatings, Wear, 209 (1997) 199-212. https://doi.org/10.1016/S0043-1648(96)07501-1.

[26] I. Apachitei, J. Duszczyk, L. Katgerman, P.J.B. Overkamp, Electroless Ni-P Composite Coatings: The Effect of Heat Treatment on the Microhardness of Substrate and Coating", Scripta Materials, 38 (1998) 1347-1353. https://doi.org/10.1016/S1359-6462(98)00054-2.

[27] Powder Diffraction File, Joint Committee on Powder Diffraction Standard (JCPDS file).

[28] S. Maheswary, S. Sharma, A. Sharma, Corrosion investigation on conventional and nanocomposite (Ni-P-Al_2O_3-TiO_2) coated Mild steel by in-plant test in digester of a paper Mill, Indian Journal of Science and Technology, 9 (2016) 1-8.

[29] S. B. Sharma, R.C. Agarwala, V. Agarwala, Dry sliding wear and friction behaviour of Ni-P-ZrO_2-Al_2O_3 composite electroless coatings on Al, International Journal of Materials Manufacturing Processing, 17 (2002) 637-649. https://doi.org/10.1081/AMP-120016088.

[30] M. Pourbaix, Atlas of Electrochemical Equilibria in Aqueous Solutions, 256; 1974, Houston, NACE.

[31] A. Sharma, V. Kumar, Behaviour of Steels against Corrosion in Peroxide Solutions, Journal of Materials and Environment Science, 3 (2011) 76-84.